PNAS

Main Manuscript for

Coordination of apicoplast transcription in a malaria parasite by internal and host cues

Yuki Kobayashi[a, 1], Keisuke Komatsuya[b, c, 1], Sousuke Imamura[a,d], Tomoyoshi Nozaki[b], Yoh-ichi Watanabe[b], Shigeharu Sato[a,e,f,g], Antony N. Dodd[h], Kiyoshi Kita[b,g,i] Kan Tanaka[a*]

[a]Laboratory for Chemistry and Life Science, Institute of Innovative Research, Tokyo Institute of Technology; Yokohama, 226-8503, Japan. [b]Department of Biomedical Chemistry, Graduate School of Medicine, The University of Tokyo; Tokyo, 113-0033, Japan. [c]Laboratory of Biomembrane, Tokyo Metropolitan Institute of Medical Science; Tokyo, 156-8506, Japan. [d]Space Environment and Energy Laboratories, Nippon Telegraph and Telephone Corporation; Tokyo, 180-8585, Japan. [e]Department of Pathology and Microbiology, Faculty of Medicine and Health Sciences, Universiti Malaysia Sabah; Sabah, 88400, Malaysia. [f]Borneo Medical and Health Research Centre, Faculty of Medicine and Health Sciences, Universiti Malaysia Sabah; Sabah, 88400, Malaysia. [g]School of Tropical Medicine and Global Health, Nagasaki University; Nagasaki, 852-8523, Japan. [h]Department of Cell and Developmental Biology, John Innes Centre; Norwich, NR4 7RU, U.K. [i]Department of Host-Defense Biochemistry, Institute of Tropical Medicine, Nagasaki University; Nagasaki, 852-8523, Japan.
[1]These authors contributed equally.

*Kan Tanaka.

Email:kntanaka@res.titech.ac.jp

Author Contributions: Y. K. designed experiments and carried out the experiments, analyzed the results, and wrote the manuscript. Ke. K. carried out the malaria parasite cultivation, microscopic observation, analyzed the results, and wrote the manuscript. S. I. carried out the ChIP analysis and analyzed the results. T. N. and Y. W. supported the malaria parasite cultivation. S. S. conducted the parasite cultivation, phylogenetic analysis and wrote the manuscript. A. D. designed experiments and wrote the manuscript. Ki. K. supervised the projects, was the project's adviser and wrote the manuscript. K. T. designed experiments, carried out the RNA polymerase σ subunit activity assay and had overall responsibility for the study and wrote the manuscript. All authors conceived the experiments, analyzed the results, and coedited the manuscript.

Competing Interest Statement: The authors declare no competing interests.

Classification: Biological science; Microbiology

Keywords: *Plasmodium falciparum,* Apicoplast, Sigma subunit, Transcriptional regulation, Melatonin.

This PDF file includes:

Main Text
Figures 1 to 4

Abstract

The malaria parasite *Plasmodium falciparum* has a non-photosynthetic plastid called the apicoplast, which contains its own genome. Regulatory mechanisms for apicoplast gene expression remain poorly understood, despite this organelle being crucial for the parasite life cycle. Here, we identify a new nuclear-encoded apicoplast RNA polymerase σ subunit (sigma factor) which, along with the α subunit, appears to mediate apicoplast transcript accumulation. This has a periodicity reminiscent of parasite circadian or developmental control. Expression of the apicoplast σ subunit gene, *apSig*, together with apicoplast transcripts, increased in the presence of the blood circadian signaling hormone melatonin. Our data suggest that the host circadian rhythm is integrated with intrinsic parasite cues to coordinate apicoplast genome transcription. This evolutionarily conserved regulatory system might be a future target for malaria treatment.

Significance Statement

Malaria is an infectious disease caused by the malaria parasite and characterized by periodic fevers. This periodicity arises from the synchronization of circadian rhythms and mitotic cycles between the host and the parasite. Here, we show that transcription within the apicoplast, an essential chloroplast-like organelle that is unique to the parasite, is regulated by both endogenous cues and by the host blood circadian hormone melatonin, *via* a novel σ^{70}-like sigma factor ApSigma. We propose a model for the melatonin signaling mechanism that regulates ApSigma. Our results suggest that the regulation of apicoplasts, which have their own genome, involves a mechanism of synchronization with the host. This novel regulatory mechanism might be a future target for malaria treatment.

Main Text

Introduction

Malaria is an infectious disease caused by infection with malaria parasite *Plasmodium falciparum*. Patients infected with malaria experience periodic cold, fever, headache, and fatigue. This periodicity is considered to occur because the parasite life cycle synchronizes with the circadian rhythms in the host. *P. falciparum* matches host circadian rhythms after infection is established, whereas it becomes asynchronous *in vitro*, suggesting the requirement for host-derived signals (1). Melatonin, a circadian control hormone secreted by the host, has proposed as a potential cue for synchronization, although it is not required (1, 2). Culture of *P. falciparum* with melatonin *in vitro* accelerates its developmental transition to the schizont stage (1). Perturbation of host and parasite rhythms during intraerythrocytic parasite development seriously affects the growth of asexual malaria parasites and their host transmission efficiency (3, 4). Therefore, understanding processes that co-ordinate parasite development with the host circadian rhythm has the potential to identify therapeutic targets.

Plasmodium falciparum and related apicomplexan parasites harbor a non-photosynthetic plastid called the apicoplast, which contains its own genome (5). The apicoplast is essential, as inhibition of apicoplast transcription, translation and replication kills the malaria parasite (6, 7). Therefore, apicoplast gene expression is a promising target for antimalarial drugs (8). In *P. falciparum* in the intraerythrocytic stage, the expression of apicoplast genes is synchronous and variable depending on parasite developmental stages (9, 10). However, little is known about the underlying mechanism for apicoplast gene expression. In plants, one mechanism that regulates plastid gene expression involves nuclear-encoded σ^{70}-like sigma subunits. These are considered to confer promoter specificity to the plastid-encoded plastid RNA

polymerase (PEP) that is similar to bacterial RNA polymerase (11, 12). We found previously that certain plant σ subunits participate in the circadian regulation of plastid gene expression in plants (13). PEP is also present in the *P. falciparum* apicoplast (14, 15), with β, β' and β''-subunits encoded by the apicoplast genome and α subunits encoded in the nucleus (*rpoA1* and *rpoA2*, amino acid alignment is shown in Fig. S1) (16, 17). We hypothesized that a nuclear-encoded σ subunit might coordinate apicoplast gene expression with the *P. falciparum* or host circadian rhythms and developmental cues.

Results

Characterization and phylogenetic analysis of ApSigma. No genes are annotated as an apicoplast σ subunit in the *Plasmodium* genome databases. Using *E. coli* σ^{70} as the basis for a sequence similarity search, we predicted that PF3D7_0621000 encodes a nuclear-encoded apicoplast σ subunit in *P. falciparum*, which we named *apSig* (gene) and ApSigma (protein; Fig. S2). σ^{70} family σ subunits have conserved regions (regions 1.1-4.2) (8, 17), which include functional domains that interact with specific DNA promoter elements and the RNA polymerase core enzyme. All these conserved regions occur in ApSigma (Fig. S2, Fig. S3). We also predicted the 3D structures of the conserved regions of ApSigma (Fig. S4). Regions 2 and 4 were highly conserved in both primary amino acid sequence and predicted 3D structure (Fig. 1A, Fig. S2, Fig. S4). These regions are important domains of the sigma subunit that recognize the -10 and -35 regions of the promoter (18, 19). The conservation of these structural similarities in ApSigma suggests that it functions as a σ subunit. ApSigma has a long N-terminal extension, which was predicted to be a transit sequence for localization to the apicoplast. To test this prediction, we generated ApSigma antibodies and performed localization analysis, which confirmed that ApSigma localizes to the apicoplast in the trophozoite, schizont, and ring stages. (Fig. 1A, Fig. S5). Therefore, the long N-terminal extension may function as the apicoplast-targeting sequence. We wished to test whether ApSigma has activity as an RNA polymerase sigma factor. We previously attempted to knock out the *P. falciparum apSig* gene, but could not isolate the mutant. We interpret this as indicating that the *apSig* gene is likely to be essential for viability. Constitutive overexpression of the *apSig* gene was also unsuccessful, which might be due to toxicity of ApSigma protein overproduction. Furthermore, bacterial-overproduced ApSigma protein was insoluble, so we could not obtain a biochemically-testable ApSigma protein. Since biochemical purification of the apicoplast RNA polymerase from *Plasmodium* sp. is not practical, we tested ApSigma activity through heterologous expression of a chimeric protein formed from ApSigma and the *E. coli* alternative sigma factor σ^S (Fig. S6A). In *E. coli*, σ^S recognizes the *katE* promoter, which shares a common -10 promoter element with other consensus-type promoters, but is not recognized by other sigma factors. Thus, in σ^S mutant *E. coli* where *katE* is not expressed, *katE* promoter activity provides a tool to test for sigma factor activity. In our chimeric protein, parts of the -10 promoter element-recognition helix (regions 2.3-2.4, (2)) of σ^S was substituted with the corresponding amino acid sequence of ApSigma (Fig. S6A). Using this, we found that the ApSigma peptide sequence responsible for promoter -10 region recognition can partially substitute the activity of the corresponding sequence of *E. coli* σ^S (Supplementary Experiment; Fig. S6B). This suggests that ApSigma has sigma factor activity, and can function as the apicoplast σ subunit.

Other species included in the apicomplexa, such as haemosporidians and coccidians, also harbor one gene that is homologous to ApSigma. Furthermore, a homolog of ApSigma is present in *Vitrella brassicaformis*, a chromerid species related to the Apicomplexa. Our phylogenetic analyses revealed that apicomplexan σ subunit proteins constitute a monophyletic clade after divergence from the chromerid protein, and each of the haemosporidian and the coccidian proteins forms independent clades within the apicomplexan clade (Fig. S7). This implies that the apicomplexan species inherited their σ subunits from a common ancestor, without horizontal gene transfer events.

ApSigma binds to the apicoplast genome. We hypothesized that if ApSigma functions as an apicoplast RNA polymerase σ subunit, it will interact specifically with DNA within apicoplast promoter regions. To examine this, 5 sites from putative promoter regions estimated from the apicoplast genome structure (R1-4 and R6) and 7 sites from other regions (R5 and R7-12) were selected. The interaction of these regions with ApSigma was analyzed by chromatin immunoprecipitation (ChIP) (Fig. 2A, Fig. S8). This found that ApSigma preferentially interacted with R1-4, 8 and 11 compared with R9, the protein-coding region with the lowest binding value, which we used as a negative control (Fig. 2B, Fig. S9). Weak interaction of ApSigma to the apicoplast genome was observed for the negative control, R9 (Fig. 2B). A recent study indicates that the σ^{70} subunit binds to bacterial RNA polymerase core and elongation complex not only during transcription initiation, but also during the elongation reaction (20). Therefore, the weak binding occurring within R9 might be this ApSigma interaction with the RNA polymerase elongation complex. We suggest that the regions R1-4, 6, and 11, which showed significantly stronger ApSigma binding than R9, are promoter regions. It was previously suggested that two long polycistronic transcripts (> 15 kb) are produced, initiating from tRNA gene clusters between the large and small subunit ribosomal RNA genes in the apicoplast genome (14). The preferential interaction of ApSigma with R1-R4 (Fig. 2B, Fig. S9) is consistent with this prediction. A significant ApSigma interaction was also identified from other sites (R6 and R11), suggesting the existence of two additional promoters or RNA polymerase pausing regions (Fig. 2A; orange arrows, Fig. S8). This is the first experimental evidence revealing the promoter locations within the *P. falciparum* apicoplast genome.

Apicoplast transcriptome accumulation is periodic. It was previously shown that *P. falciparum* retains its own circadian rhythm to facilitate intraerythrocytic development (20). Given that circadian rhythms of chloroplast gene expression in plants are regulated by nuclear-encoded PEP subunits (13), we hypothesized that a similar mechanism could be present in *P. falciparum*. To investigate this, we extracted the transcriptional profiles of *P. falciparum* in erythrocytes from published microarray analyses (9, 10) (Fig. 2C, S10A). Using this, we identified with periodicity-detecting algorithms (JTK_CYCLE, Lomb-Scargle) (21) that all apicoplast genes are expressed periodically (Bonferroni-Hochberg adjusted $P < 0.01$ for all genes, in both datasets) (BH.Q in Table S1, S2). In one dataset (9), accumulation of about 70% and 30% of the gene transcripts had estimated periods of 48 h and 24 h, respectively (Fig. 2C, S10B, C, Table S1). In another dataset (10), only transcripts with a 48 h period were detected (Table S2). The 48 h-period transcript set peaked in abundance at the early schizont stage in both datasets. We found that the nuclear *apSig* transcript also had a 48 h period, but its phase of oscillation preceded the apicoplast genes by 7-8 h, and peaked at the early to mid-trophozoite stage. Interestingly, transcripts for the apicoplast RNA polymerase α subunit genes, *rpoA1* and *rpoA2*, encoded in the nucleus, had high correlation coefficients with apicoplast transcripts having a 48 h period, which may indicate a mechanism to synchronize the apicoplast and nuclear gene expression (Table S3).

Melatonin-responsiveness of both *apSig* and apicoplast transcripts. The mammalian hosts of malaria parasites have their own circadian rhythm, and the rhythm is communicated across their body through mechanisms including the blood hormone melatonin. Given the periodicity of *apSig* and apicoplast transcript accumulation (Fig. 2C), we were interested in the coordination of parasite gene expression programs with melatonin levels. We examined this, focusing on the nuclear encoded apicoplast σ subunit ApSigma. For this, accumulation of protein-coding apicoplast transcripts in trophozoite cells was examined after 30 or 90 minutes of melatonin treatment. Melatonin is present in human blood up to about 200 pM (23). We performed a preliminary experiment with 200 pM and detected increased *apSig* transcripts (Fig. S11). However, the stability of reproduction under experimental conditions was poor, so we used 10 nM melatonin, as reported by Furuyama et al. (24), because this gave consistent and reproducible results. The *apSig* transcripts and the apicoplast gene transcripts *sufB*, *rpoC2* and *tufA* accumulated in response to melatonin, suggesting that melatonin positively regulates apicoplast gene expression through ApSigma function (Fig. 3A). The increase in *apSig* transcripts was specific, because nuclear encoded *act1* and

rpoA1/2 genes encoding actin and apicoplast RNA polymerase α subunits, respectively, were unchanged. SufB is a protein involved in the biosynthesis of iron-sulfur clusters that drive the methylerythritol phosphate (MEP) pathway for isoprenoid synthesis, which is essential for malaria parasite survival (25). In addition to the apicoplast *sufB* gene, nuclear encoded *sufC* and *sufD* gene transcripts for the FeS cluster biosynthetic enzyme SufBCD (6), and those of *ispG* and *ispH*, encoding key enzymes of the MEP pathway (25), were increased by melatonin (Fig. S12). This suggests that MEP pathway activity in the apicoplast was affected by the host circadian rhythm. In contrast, expression of the apicoplast transcript *rpl4* did not respond to melatonin. Therefore, multiple transcriptional regulatory mechanisms might exist for apicoplast gene transcription.

To further understand the interaction and coordination between the parasite and host rhythmicity, we examined whether there is circadian or developmental gating of the response of *apSig* expression and apicoplast transcription to melatonin. Melatonin was administered at various times during synchronous culture, with cells sampled to investigate the melatonin response of *apSig, sufB* and *act1* transcripts (Fig. 3B). Melatonin had a time-restricted effect, inducing *apSig* and *sufB* prominently at 22h-24h after synchronization, after which the response decreased (Fig. 3B). This change in melatonin sensitivity over time might be due to circadian gating of the response, or developmental stage-specific sensitivity. Together, this suggests that extrinsic circadian cues, intrinsic circadian cues and developmental timing cues are integrated to coordinate the transcription of the apicoplast genome (Fig. 4).

The melatonin response signaling pathway for *apSig*. Finally, we investigated the mechanism of activation of *apSig* expression in response to melatonin. Two distinct pathways are considered to mediate melatonin signaling in *P. falciparum* (Fig. 3C) (26). One is the inositol trisphosphate (IP_3) pathway *via* phospholipase C (PLC), and another is the cAMP pathway *via* adenylyl cyclase (AC). We analyzed the melatonin response of *apSig* and apicoplast *sufB* genes in the presence of the melatonin receptor inhibitor luzindole, the PLC inhibitor U73122, or the AC inhibitor MDL12330. Since melatonin-induced transcript elevation occurred also in non-synchronized cultures, this experiment was performed under non-synchronized conditions. In this experiment with non-synchronized cells, melatonin caused approximately 1.5-fold increase of *apSig* and *sufB* transcripts (Fig. 3D). This response was inhibited by luzindole or MDL12330, whereas U73122 had no effect (Fig. 3D). Furthermore, cAMP addition mimicked the effect of melatonin (Fig. 3D). Together, these results suggest that melatonin induces *apSig* gene expression through the second messenger cAMP, which results in the upregulation of apicoplast gene expression.

Discussion

We identified a nuclear-encoded *E. coli* σ^{70} homolog, ApSigma, in a *P. falciparum*. This has highly conserved primary sequence and 3D structure of its core enzyme binding sites and promoter recognition sites. Furthermore, we found that ApSigma binds to apicoplast DNA *in vivo* (Fig 2A, B) and has conserved domains that can participate in promoter recognition (Fig S6A, B). Together, this strongly suggests that ApSigma, like the sigma subunit of PEP in plants, regulates apicoplast transcription. In plants, plastid transcription by PEP is regulated by changes in the expression of the sigma subunits in response to the external environment and tissue differentiation (11-13). We hypothesized that in parasites, ApSigma expression is regulated by signals in the host blood, thereby controlling apicoplast gene expression. We determined that melatonin, a host blood hormone, elevates *apSig* transcripts and this correlates with changes in apicoplast encoded transcripts. In contrast, transcripts of the nuclear-encoded *rpoA1,2* subunits were unresponsive to melatonin (Fig 3A). This suggests that the melatonin-stimulated increase in apicoplast transcription is ApSigma-dependent. These observations suggest that the mechanism by which the external environment regulates plastid gene expression, *via* the σ subunit, is evolutionarily conserved in malaria parasites.

We identified periodicity in apicoplast gene expression (Fig. 2C, Fig S10, Table S1, S2). However, this periodicity did not correlate with the *apSig* expression. This suggests that ApSigma might not be involved in determining the periodicity of apicoplast transcription in the absence of host cues. In contrast, both nuclear-encoded *rpoA1*, *2* are regulated by the

circadian clock (21), and their expression patterns correlated very highly with apicoplast gene expression (Table S3). One interpretation is that the *rpoA*s might underlie the periodicity of apicoplast transcription. Our observations suggest that the periodicity of apicoplast transcription is driven by internal parasite cues such as intrinsic circadian rhythms, whereas ApSigma regulates apicoplast gene expression in response to melatonin from the host cues. This suggests that external and internal timing cues are integrated to regulate apicoplast genome transcription.

Since the apicoplast is integral to the cell, its development is strictly synchronized with the cell cycle. Detailed microscopic observations have reported the morphological dynamism of the apicoplast at each stage of parasite development (27). It is thought that specific molecular mechanisms align the morphology and metabolism of the apicoplast with the parasite life cycle (27). This might involve the processes that regulate expression of apicoplast *sufB*, which is one of the few essential genes encoded by the apicoplast genome. SufB-containing complexes supply FeS clusters to the MEP pathway for isoprenoid synthesis, which is essential for malaria survival (28-30). This implies that maintenance of *sufB* expression from the apicoplast genome is essential for parasite survival. We have shown that induction of *apSig* by melatonin upregulates *sufB* transcription (Fig. 3A). We also found that the expression of both apicoplast *sufB* and nuclear encoded *sufC*, *sufD*, *ispG*, and *ispH* were upregulated by the addition of melatonin (Fig. S12). This suggests that *apSig* may form part of the mechanism that aligns the apicoplast with the parasite developmental cycle.

Interestingly, we found that the melatonin-induced upregulation of *apSig* expression is restricted to the trophozoite stage only (Fig. 3B). This might result from coordination between the synchronized regulatory system of parasite developmental stage with apicoplast function and the signal from the host. Perhaps the provision of a parasite differentiation timing-specific FeS cluster and activation of the MEP pathway contributes to synchronization of the parasite with the apicoplast, and some mechanisms restrict the activation of apicoplast transcription by host signals in a time-specific manner. We suggest that *apSig* expression involves a sophisticated regulatory system that integrates the timing of parasite differentiation, circadian rhythms, synchronization with the apicoplast, and signals from the host.

We propose a regulatory scheme whereby the endogenous parasite rhythm is transmitted to the apicoplast and that the melatonin-mediated host rhythm modulates apicoplast transcriptional activity through the regulation of the ApSigma (Fig. 4). A mitochondria-targeting drug called atovaquone is known to be an effective antimalarial, and the apicoplast could also be a promising target for the drug development (31, 32). The Apicomplexan plastid σ subunit homologs and apicoplast transcriptional regulation, identified here, represent new potential targets for treatment and prevention of both malaria and infections caused by other apicomplexan parasites such as Toxoplasma and other coccidia.

Among rodent-parasitizing *Plasmodium* species, *P. chabaudi* and *P. vinckei* have a 24-hour cycle in which they propagate synchronously, whilst *P. berghei* and *P. yoelii* have 18- and 21-hour cycles, respectively, in which they propagate asynchronously (33, 34, 35). The mitotic rhythm of *P. chabaudi* is determined by the host rhythm, whereas that of *P. vinckei* is found to be partially independent of the host (33). It has also been reported that growth of *P. chabaudi* is highly synchronous even in mice lacking melatonin production, such as C57BL/6J mice (2). The duration and degree of synchrony of the growth of the parasite is expected to be determined by the unknown endogenous cycle-regulation mechanism that functions in each *Plasmodium* species after its activation responding to a trigger from external melatonin. Even if the timing of switch-on by the trigger (melatonin) in the host is invariant, the length of time between each subsequent small event may vary, which may or may not cause a significant fluctuation in the length of time between each event. It is not surprising that a variety of responses could have evolved in different species, depending on infection strategy. As a result, some *Plasmodium* species may have cycles of different lengths, and others may have different degrees of synchrony. However, melatonin cues are unlikely the only factors that define the cell cycles of the parasites, with multiple other signals that probably depend on each host and *Plasmodium* species also likely involved. Further studies are needed to explain the cell cycle regulation mechanism in *Plasmodium* comprehensively.

Materials and Methods

Malaria parasite cultivation. *P. falciparum* strain 3D7 was cultured at 3% hematocrit with type A+ human erythrocytes in RPMI 1640 medium (Thermo Fisher Scientific, Waltham, USA), supplemented with 25 mM $NaHCO_3$, 10 μg/mL gentamicin sulphate, 10 μg/mL hypoxanthine, 25 mM HEPES, 0.8 mg/mL L-glutamine, and 0.5 % (w/v) Albumax II (Thermo Fisher Scientific)(36). Cultures were maintained under 5% O_2, 5% CO_2, and 90% N_2 at 37℃. Parasitemia was determined with thin blood smears stained with Giemsa. The experiments using human erythrocytes were performed under the guidelines of the ethical committee of the University of Tokyo (#10050-(2)). Human erythrocytes were obtained from Japanese Red Cross Society (No.25J0207). Synchronization of the parasite cultures was performed by 5 % (w/v) sorbitol treatment for 10 minutes (37).
For analysis of effect of melatonin on the parasite, erythrocytes infected by late trophozoites and schizonts were collected using 63% (v/v) Percoll density centrifugation (38) from parasite cultures pre-treated with 5% (w/v) sorbitol (39). After an incubation for 4 hours, the Percoll-purified erythrocytes were treated with 5% (w/v) sorbitol and removed trophozite and schizont stages. After an incubation for 22 hours, the erythrocytes with parasites highly synchronized to early trophozoite stage were incubated with or without 10 nM melatonin (Sigma-Aldrich, Burlington, USA) for 30 or 90 minutes. After the treatment, erythrocytes were collected by centrifugation, washed with phosphate buffered saline (PBS), and stored at -80°C until use.
For analysis of signal transduction in the parasite, erythrocytes infected by early trophozoites were treated with luzindole (melatonin receptor inhibitor; Sigma-Aldrich) (22), 1 μM MDL12330A (adenylate cyclase inhibitor; Sigma-Aldrich) (22), 10 μM U73122 (PLC inhibitor; Tocris Bioscience, Bristol, UK) (23), or no inhibitor, for 90 min at 37℃. Subsequently, parasite cultures were incubated with 10 nM melatonin for 90 min at 37℃. After incubation, parasite cultures were then pelleted by centrifugation, washed by PBS, and stored at -80°C until use.

Phylogenetic analysis. Apicomplexan σ subunits in the amino acid sequence database were searched for by BLAST analysis at PlasmoDB (https://plasmodb.org/plasmo/app), using conserved domain sequence of σ^{70} of *E. coli* (BAB37373) as the query. One σ subunit-like sequence was identified in each of *P. falciparum* 3D7 (XP_966194.1 encoded by PF3D7_0621000), *Eimeria brunetti* (CDJ52515), *Eimeria necatrix* (XP_013434793), *Eimeria maxima* (XP_013337375), *Cyclospora cayetanensis* (XP_026192347), *Toxoplasma gondii* VEG (ESS33313), *Toxoplasma gondii* CAST (RQX72928), *Neospora caninum* (XP_003881399), *Plasmodium berghei* (XP_034422407), *Plasmodium vivax* (SCO73651), *Plasmodium relictum* (XP_028533929) and *Vitrella brassicaformis* (CEL93836). Amino acid sequences (region 2-4) were aligned using ClustalW, and the alignment was refined by eye. Phylogeny of the σ subunits was analyzed by maximum likelihood method using MEGA program, and bootstrap values were calculated replicating 1000 analyses with LG+G model. In the gregarines and piroplasmids, no σ subunit homologs are not identified. In gregarines, the apicoplast is lost (40, 41). The structure of the apicoplast genome of piroplasmids differs from the general plastid genome because all genes, including those of rRNAs and tRNAs, occupy one strand of the genome (42). Probably, a different mechanism that does not involve σ subunit regulates apicoplast gene expression in piroplasmids.

Prediction of 3D structure. For ApSigma structural predictions, we used a version of AlphaFold (version 2) available at https://colab.research.google.com/github/sokrypton/ColabFold/blob/main/AlphaFold2.ipynb. that allows single predictions (43). The PDB file output from AlphaFold was visualized, edited and colored with UCSF Chimera (44).

Preparation of anti-ApSigma antibody. A 654 nt-long synthetic DNA fragment encoding the 2.4 region of ApSigma in a modified codon usages that matches the one of highly expressed proteins of *E. coli* (Table S4), and another fragment with the complementary sequence, were obtained from Azenta (Chelmsford, UK). The double strand DNA fragment composed from the two fragments was inserted into *Sma*I-digested pGEX-4T-1 (GE Healthcare, Chicago, USA). Expression of the recombinant proteins in *E. coli* and their purification were performed

as described previously (45). A Guinea pig was immunized with the recombinant protein and polyclonal antibodies against ApSigma were purified by Tanpaku Seisei Kougyou (Isezaki, Japan).

Immunofluorescence microscopy. Human erythrocytes infected by *P. falciparum* were fixed in 2% (w/v) paraformaldehyde containing 0.075% (w/v) glutaraldehyde in PBS for 10 min. The reaction was quenched using 0.1 M glycine in PBS for 15 min. After blocking in 3% (w/v) bovine serum albumin (BSA), 0.2 % (w/v) Tween 20 in PBS for 1 hour, the erythrocytes were incubated with anti-ApSigma antibody (diluted 1:200) and rabbit anti-HU antibody (diluted 1:200) or rabbit anti-ATG8 antibody (a kind gift from Dr. Noboru Mizushima, The University Tokyo, diluted 1:200) in 1% BSA, 0.2% (v/v) Tween 20 in PBS for 1 hour (46, 47). Then, erythrocytes were washed in 0.2% (v/v) Tween 20 in PBS three times and incubated with Alexa Flour 561-conjugated goat anti-guinea pig IgG (1:1000) and Alexa Flour 488-conjugated goat anti-rabbit IgG (1:1000) for 1 hour. The fluorescence images were captured by a confocal microscopy system with Zeiss LSM780 and LSM980 (Carl Zeiss, Oberkochen, Germany).

ChIP analysis. Erythrocytes infected by *P. falciparum* 3D7 at high parasitemia (above 10%) were collected from 20 ml cultures by centrifugation at 800×g for 5min at room temperature. The collected cells with parasites were fixed with 1% (v/v) formaldehyde at 37 ºC for 10 min, followed by 0.125 M glycine for 5 min. The fixed erythrocytes were incubated in PBS containing saponin (0.075% (w/v)) and released parasites were collected by centrifugation. After washes with PBS buffer, the parasites were stored at -80°C until use. The parasites were resuspended in 0.5 mL ChIP lysis buffer (50 mM Tris-HCl, 140 mM NaCl, 1 mM EDTA, 0.1% (w/v) SDS, 1 % (v/v) Triton X100, 0.1 % (w/v) Sodium Deoxycholate, Complete Mini (Sigma-Aldrich), EDTA-free, protease inhibitor, pH 8.0), and cell disruption and shearing of genomic DNA were achieved by sonication (Branson Sonifier 250 (Emerson Electric, St. Louis, USA), Duty Cycle 50, Output Control 2.0, 20 sec, 10 times). After sonication, it was experimentally confirmed that the size of genomic DNA fragments was within the range of 100 and 300 bp. The sonicated parasite suspension was centrifuged and the supernatant containing the fragmentated genomic DNA was collected. To a 0.4 ml of the collected supernatant, a 19-fold volume of ChIP lysis buffer was added, and pretreated with nProtein A Sepharose 4 Fast Flow (Sigma-Aldrich) for 4 hr at 4 ºC. After removal of nProtein A Sepharose beads by column filtration, the collected solution was divided into 2. Each of these was subjected to immunoprecipitation. Immunoprecipitations were performed with 5.0 μl of crude serum containing anti-ApSigma antibody or the preimmune serum at 4 ºC overnight, then a 30 μl of 50 % (v/v) slurry of magnetic Dynabeads (Thermo Fisher Scientific). Protein was added before further incubated for 5 hours. The beads were washed twice with each of: RIPA150 buffer (50 mM Tris-HCl, 150 mM NaCl, 1 mM EDTA, 1% (v/v) Triton X-100, 0.1% (v/v) SDS, 0.1% (v/v) sodium deoxycholate, pH 8.0), RIPA500 buffer (50 mM Tris-HCl, 500 mM NaCl, 1 mM EDTA, 1% (v/v) Triton X-100, 0.1% (v/v) SDS, 0.1% (v/v) sodium deoxycholate, pH 8.0), LiCl wash solution (10 mM Tris-HCl, 250 mM LiCl, 1 mM EDTA, 0.5% (v/v) Nonidet P40, 0.5% (w/v) sodium deoxycholate, pH 8.0), and TE buffer: in this order. For reversions of the cross-link, the beads were resuspended in ChIP direct elution buffer (10 mM Tris-HCl, 300 mM NaCl, 5 mM EDTA, 0.5% (v/v) SDS, pH 8.0) and incubated at 65°C overnight. After a treatment with RNase A and proteinase K, DNA was extracted from the beads using phenol:chloroform:isoamylalcohol (25:24:1) and precipitated with ethanol using Ethachinmate (Nippon Gene, Tokyo, Japan) as a carrier. The resultant pellets were dissolved in 100 ml of water and analysed by qPCR using relevant sets of primers (Table S5), as reported previously (48) with modifications. Briefly, amplifications were done by incubating reaction mixtures at 95°C for 2 min prior to 40 cycles of 10 sec at 95°C followed by 15 sec at 40°C and 30 sec at 60°C. Standard curves were constructed with several serial dilutions (1 to 1×10^{-4}) of input DNA to estimate percent of input of each DNA fragment relative to the input DNA.

Detection of periodicity in gene expression. We used MetaCycle in R package (https://cran.r-project.org/web/packages/MetaCycle/MetaCycle) with the JTK_CYCLE and

Lomb-Scargle algorithms (20, 49, 50) to detect periodicity of a length between 20 and 48h in the expression profiles of the transcripts from the gene.

RT-qPCR analysis. Total RNA was isolated from the parasites infecting the erythrocytes with Trizol LS reagent (Thermo Fisher Scientific), according to manufacturer's instructions. First-strand synthesis of cDNA was performed using 1 μg RNA and ReverTra Ace qPCR RT Master Mix with gDNA Remover (Toyobo, Osaka, Japan) according to manufacturer's instructions. The abundance of each transcript was quantified by qPCR. qPCR was performed as described (45), using primers shown in Table S6. Expression of each gene was normalized with the value of 18S rRNA. A Shapiro-Wilk test was performed on all data groups after analysis. All data groups had P>0.05, so Student's *t-test* was performed to determine significant differences.

Acknowledgments

The authors thank Dr. Noboru Mizushima for providing the Anti-PfATG8 antibody, the Materials Analysis Division, Open Facility Center, Tokyo Institute for Technology for DNA sequence analysis. This work was supported by MEXT/JSPS KAKENHI (20K06638), Grant-in-Aid for JSPS Research Fellow No. 15J04920, Ohsumi Frontier Science Foundation, BBSRC (UK) Institute Strategic Program GEN BB/P013511/1 and BRiC BB/X01102X/1, Tokyo Institute of Technology World Research Hub Initiative (WRHI) Program of Institute of Innovative Research, Nagasaki University "Doctoral Program for World-leading Innovative and Smart Education" for Global Health, "Global Health Elite Programmed for Building a Healthier World" from MEXT.

References

1. CT Hotta, et al., Calcium-dependent modulation by melatonin of the circadian rhythm in malarial parasites. *Nat. Cell Biol.* **2**, 466–468 (2000).
2. F Rijo-Ferreira et al. The malaria parasite has an intrinsic clock. Science. 368, 746-753 (2020).
3. AJ O'Donnell, N Mideo, SE Reece. Disrupting rhythms in *Plasmodium chabaudi*: Costs accrue quickly and independently of how infections are initiated. *Malar. J.* **12**, 372 (2013).
4. AJ O'Donnell, P Schneider, HG McWatters, SE Reece. Fitness costs of disrupting circadian rhythms in malaria parasites. *Proc. Biol. Sci.* **278**, 2429–2436 (2011).
5. GI McFadden, The apicoplast. *Protoplasma*. **248**, 641–650 (2011).
6. ZR Pala, V Saxena, GS Saggu, S Garg, Recent advances in the [Fe–S] cluster biogenesis (SUF) pathway functional in the apicoplast of *Plasmodium*. *Trends Parasitol*. **34**, 800–809 (2018).
7. E Yeh, JL DeRisi, Chemical rescue of malaria parasites lacking an apicoplast defines organelle function in blood-stage *Plasmodium falciparum*. *PLoS Biol.* **9**, e1001138 (2011).
8. A Chakraborty, Understanding the biology of the *Plasmodium falciparum* apicoplast; an excellent target for antimalarial drug development. *Life Sci.* **158**, 104–110 (2016).
9. HJ Painter et al., Genome-wide real-time in vivo transcriptional dynamics during *Plasmodium falciparum* blood-stage development. *Nat. Commun*. **9**, 2656 (2018).
10. Z Bozdech et al., The transcriptome of the intraerythrocytic developmental cycle of *Plasmodium falciparum. PLoS Biol*. **1**, e5 (2003).
11. K Kanamaru, K Tanaka, Roles of chloroplast RNA polymerase sigma factors in chloroplast development and stress response in higher plants. *Biosci. Biotechnol. Biochem*. **68**, 2215–2223 (2004).
12. J Schweer, H Türkeri, A Kolpack, G Link, Role and regulation of plastid sigma factors and their functional interactors during chloroplast transcription - recent lessons from *Arabidopsis thaliana*. *Eur. J. Cell Biol.* **89**, 940–946 (2010).
13. ZB Noordally et al., Circadian control of chloroplast transcription by a nuclear-encoded timing signal. *Science* **339**, 1316–1319 (2013).
14. J Li, JA Maga, N Cermakian, R Cedergren, JE Feagin, Identification and characterization of a *Plasmodium falciparum* RNA polymerase gene with similarity to mitochondrial RNA polymerases. *Mol Biochem Parasitol*. **113**, 261–269 (2001).

15. RE. Nisbet, JL McKenzie, Transcription of the apicoplast genome. *Mol. Biochem. Parasitol*. **210**, 5-9 (2016).
16. EL. Dahal, PJ. Rosenthal, Apicoplast translation, transcription and genome replication: targets for antimalarial antibiotics. *Trends Parasitol*. **24**, 279-284 (2008)
17. MS Paget, Bacterial sigma factors and anti-sigma factors: structure, function and distribution. *Biomolecules.* **5**, 1245-1265 (2015).
18. U Mechold, K Potrykus, H Murphy, KS Murakami, M Cashel, Differential regulation by ppGpp versus pppGpp in *Escherichia coli*. *Nucleic Acids Res.* **41**, 6175-6189 (2013).
19. GA Patikoglou et al., Crystal structure of the *Escherichia coli* regulator of sigma70, Rsd, in complex with sigma70 domain 4. *J. Mol. Biol*. **372**, 649-659 (2007).
20. I Petushkov, D Esyunina, A Kulbachinskiy. Possible roles of σ-dependent RNA polymerase pausing in transcription regulation. *RNA Biol*.**14**, 1678-1682 (2017).
21. LM Smith et al., An intrinsic oscillator drives the blood stage cycle of the malaria parasite *Plasmodium falciparum*. *Science*. **368**, 754–759 (2020).
22. G Wu, RC Anafi, ME Hughes, K Kornacker, JB Hogenesch, MetaCycle: an integrated R package to evaluate periodicity in large scale data. *Bioinformatics*. **32**, 3351–3353 (2016).
23. A Dawn et al., The central role of cAMP in regulating *Plasmodium falciparum* merozoite invasion of human erythrocytes. *PLoS Pathog.* **10**, e1004520 (2014).
24. GS Richardson. The human circadian system in normal and disordered sleep. *J. Clin. Psychiatry.* **66**, 3–9 (2005).
25. T Masini, AK Hirsch, Development of inhibitors of the 2C-methyl-D-erythritol 4-phosphate (MEP) pathway enzymes as potential anti-infective agents. *J. Med. Chem.* **57**, 9740-9763 (2014)
26. W Furuyama et al., An interplay between 2 signaling pathways: melatonin-cAMP and IP_3–Ca2+ signaling pathways control intraerythrocytic development of the malaria parasite *Plasmodium falciparum*. *Biochem Biophys Res Commun.* **446**,125–131 (2017).
27. A Elaagip, S Absalon, A Florentin, Apicoplast Dynamics During *Plasmodium* Cell Cycle. *Front. Cell Infect Microbiol*. **12**, e864819 (2022).
28. KE Ellis, B Clough, JW Saldanha, RJ Wilson, Nifs and Sufs in malaria. *Mol. Microbiol.* **41**, 973–981 (2001).
29. FW Outten, O Djaman, G Storz, A suf operon requirement for Fe-S cluster assembly during iron starvation in Escherichia coli. *Mol. Microbiol.* **52**, 861–872 (2004).
30. JE Gisselberg, et al., The Suf iron-sulfur cluster synthesis pathway is required for apicoplast maintenance in malaria parasites. *PLOS Pathogens*. **9**, e1003655 (2013).
31. CD Goodman et al., Parasites resistant to the antimalarial atovaquone fail to transmit by mosquitoes. *Science.* **352**, 349–353 (2016).
32. LM. Low, DI Stanisic, MF. Good, Exploiting the apicoplast: apicoplast-targeting drugs and malaria vaccine development. *Microbes Infect*. **20**, 477–483 (2018).
33. CR Garcia, RP Markus, L Madeira. Tertian and quartan fevers: temporal regulation in malarial infection. *J. Biol. Rhythms* **16**, 436–43 (2001).
34. AJ O`Donnell, SE Reece. Ecology of asynchronous asexual replication: the intraerythrocytic development cycle of Plasmodium berghei is resistant to host rhythms. *Malar. J*. **20**, 105 (2021).
35. P Gautret, E Deharo, AG Chabaud, H Ginsburg, I Landau. *Plasmodium vinckei vinckei, P. v. lentum and P. yoelii yoelii:* chronobiology of the asexual cycle in the blood. *Parasite.* **1**, 235-239 (1994).
36. W Trager, J Jensen, Human malaria parasites in continuous culture. *Science.* **193**, 673–675 (1976).
37. C Lambros, JP Vanderberg, Synchronization of *Plasmodium falciparum* erythrocytic stages in culture. *J Parasitol.* **65**, 418–420 (1979).
38. CE Tosta, M Sedegah, DC Henderson, N Wedderburn, *Plasmodium yoelii* and *Plasmodium berghei*: isolation of infected erythrocytes from blood by colloidal silica gradient centrifugation. *Exp Parasitol.* **50**, 7-15 (1980).
39. XL Pang, T Mitamura, T Horii, Antibodies reactive with the N-terminal domain of *Plasmodium falciparum* serine repeat antigen inhibit cell proliferation by agglutinating merozoites and schizonts. *Infect Immun.* **67**, 1821–1827 (1999).
40. V Mathur et al., Multiple independent origins of Apicomplexan-Like parasites. *Curr. Biol.* **29**, 2936–2941 (2019).

41. MA Toso, CK Omoto, Gregarina niphandrodes may lack both a plastid genome and organelle. *J. Eukaryot. Microbiol*. **54**, 66-72 (2007).
42. Q Liu et al., Annotation and characterization of Babesia gibsoni apicoplast genome. *Parasit Vectors.* **13**, 209 (2020).
43. J Jumper et al., Highly accurate protein structure prediction with AlphaFold. *Nature* **596**, 583–589 (2021).
44. EF Pettersen et al., UCSF Chimera—A visualization system for exploratory research and analysis. *J. Comput. Chem.* **25**, 1605–1612 (2004).
45. Y Kobayashi, S Imamura, M Hanaoka, K Tanaka, A tetrapyrrole-regulated ubiquitin ligase controls algal nuclear DNA replication. *Nature Cell Biol.* **13**, 483-487 (2011).
46. N Sasaki et al., The *plasmodium* HU homolog, which binds the plastid DNA sequence-independent manner, is essential for the parasite's survival. *FEBS Letters*. **583**, 1446–1450 (2009).
47. K Kitamura, C Kishi-Itakura, T Tsuboi, S Sato, K Kita, N Ohta, N Mizushima. Autophagy-related Atg8 localizes to the apicoplast of the human malaria parasite Plasmodium falciparum. *PLoS One* **7**, e42977 (2012).
48. S Imamura et al., The checkpoint kinase TOR (target of rapamycin) regulates expression of a nuclear-encoded chloroplast RelA-SpoT homolog (RSH) and modulates chloroplast ribosomal RNA synthesis in a unicellular red alga. *Plant J*. **94**, 327-339 (2018).
49. ME Hughes, JB Hogenesch, K. Kornacker, JTK-CYCLE: An efficient nonparametric algorithm for detecting rhythmic components in genome-scale data sets. *J. Biol. Rhythms.* **25**, 372–380 (2010).
50. EF Glynn, J Chen, AR Mushegian, Detecting periodic patterns in unevenly spaced gene expression time series using Lomb-Scargle periodograms. *Bioinformatics*. **22**, 310–316 (2006).

Figures

Fig. 1. ApSigma is apicoplast-localized and has conserved domain structure representative of σ^{70} sigma factors. (A) Structural comparison of ApSigma. Comparison of the predicted 3D structure of ApSigma with the results of x-ray structural analysis of regions 2 and 4 in *E. coli* σ^{70}. The 3D structure of ApSigma was predicted using AlphaFold. Regions 2 and 4 of *E. coli* σ^{70} were extracted from the protein database file (region2 from 4jk1, region 4 from 2p7v) with the UCSF Chimera software, and compared with predicted ApSigma. The predicted 3D structure of total length of ApSigma is shown in Fig. S4. (B) Subcellular localization of ApSigma in fixed schizont-stage cells. ApSigma (red) was visualized with an anti-ApSigma antibody and Alexa Fluor 561-conjugated secondary antibody. The apicoplast localized marker ATG8 (green) was visualized with an anti-ATG8 antibody and Alexa Fluor 488-conjugated secondary antibody. DNA was stained with Hoechst (blue). The ApSigma and ATG8 images are shown separately, and also merged. Scale bar (bottom right), 10 μm.

Fig. 2. *P. falciparum* σ subunit ApSigma binds to the apicoplast genome. (A) *P. falciparum* apicoplast genome map. Small dots indicate candidate promoter regions for ChIP analysis. Red dots indicate strong ApSigma-binding regions, and blue dots indicate weak binding regions. Bold lines indicate inverted repeats (IR). Orange arrows indicate the transcription units we predicted from ChIP analysis. Fig. S8 provides a detailed genome map. (B) ChIP of ApSigma binding performed using ApSigma antibody, and preimmune serum as a control. The nuclear-encoded *BIP* (PF3D7_0917900) and *LDH* (PF3D7_1324900) genes were used as negative controls. The x-axis R value identifies the regions represented by dots on (A). Immunoprecipitated DNA was quantified by qRT-PCR using primers flanking the dots on (A). On (B), values indicate the ratio of ApSigma/preimmune serum. Student's *t*-tests compare the lowest binding region (R9, Significant differences ($P < 0.05$) are indicated by asterisk) with other regions (+/- standard deviation; n=3). (C) Expression profiles of apicoplast genes and nuclear-coded apicoplast transcription-related factors in erythrocytes from microarray data. This summarizes representative genes for clarity, with all genes shown in Fig. S10. Values indicate relative level of RNA accumulation. The differentiation stages of the parasite in erythrocytes are shown above the graph.

Fig. 3. Melatonin regulates apicoplast transcription. (A) Response of apicoplast transcription-related transcripts to melatonin. Melatonin was added to the parasite cells synchronized to the trophozoite phase, at a final concentration of 10 nM. Cells were sampled 30 min and 90 min after melatonin addition, with transcript accumulation measured using RT-qPCR. Transcript levels compared using the ratio of transcript abundance in the presence and absence of melatonin (DMSO control), to control for underlying fluctuations (+/- standard deviation; n=3). Significant differences (Student's *t*-test, $P < 0.05$) are indicated by asterisk. Genes for the nuclear and apicoplast codes are shown in blue and green, respectively. (B) Melatonin was added to parasite cells in synchronized culture at the indicated times and sampled 30 min and 90 min after addition. RNA was used for RT-qPCR and the change in expression of *apSig, sufB* and control *act1* was plotted. The top panel shows the differentiation stage of the parasite in erythrocytes. Data are n=3, +/- standard deviation. Significant differences (Student's *t*-test, $P < 0.05$) are indicated by asterisk. Genes for the nuclear and apicoplast codes are shown in green and blue, respectively. (C) Hypothesized signaling pathways for melatonin-induced *apSig* expression. Two melatonin signaling pathways are proposed, through IP_3 or cAMP, with either potentially involved in regulating *apSig* expression. (D) Effect of chemicals targeting melatonin signaling pathway on *apSig* and apicoplast gene expression. Various reagents were added to the non-synchronized culture system, and RT-qPCR detected the abundance of each transcript after 90 min. The ratios of reagent added/control (DMSO) were plotted. Standard deviations are indicated by error bars (n=3). Significant differences (Student's *t*-test, $P < 0.05$) are indicated by asterisk. Genes for the nuclear and apicoplast codes are shown in green and blue, respectively.

Fig. 4. Potential mechanism of regulation of periodic apicoplast gene expression. Apicoplast gene expression has a periodicity. This periodicity is transmitted by the rhythmic expression of *rpoA1, 2 and apSig* by the intrinsic *P. falciparum* circadian oscillator. In combination, host cues regulate the parasite rhythm. An increase in host melatonin concentration is sensed by melatonin receptors. This signal upregulates ApSigma expression via cAMP. This increased ApSigma expression may lead to the regulation of periodicity of apicoplast gene expression. The effects of melatonin in this process are influenced by parasite circadian rhythm or developmental stage. Melatonin increases the transcript of *sufB* encoded by apicoplast DNA and similarly increases the transcripts of *sufC*, *sufD*, *ispG* and *ispH* required for the MEP pathway. The activity of the MEP pathway is probably influenced by the host circadian rhythm.

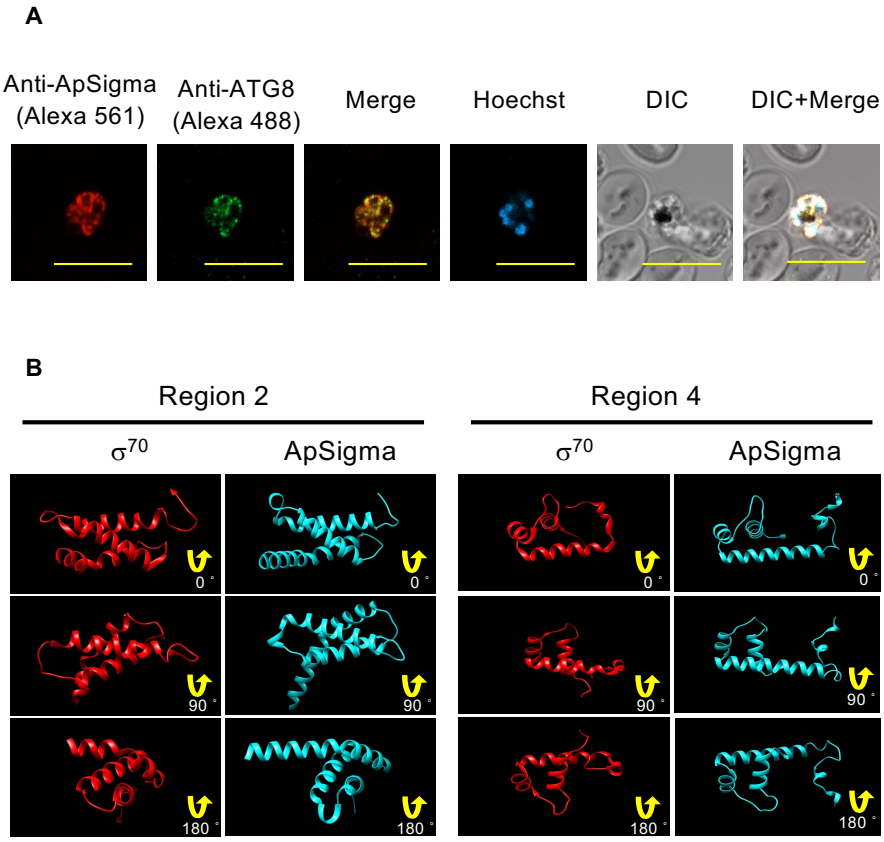
A
Anti-ApSigma (Alexa 561)
Anti-ATG8 (Alexa 488)
Merge
Hoechst
DIC
DIC+Merge
B
Region 2
Region 4
σ70
ApSigma
σ70
ApSigma
0 °
90 °
180 °

Fig. 1

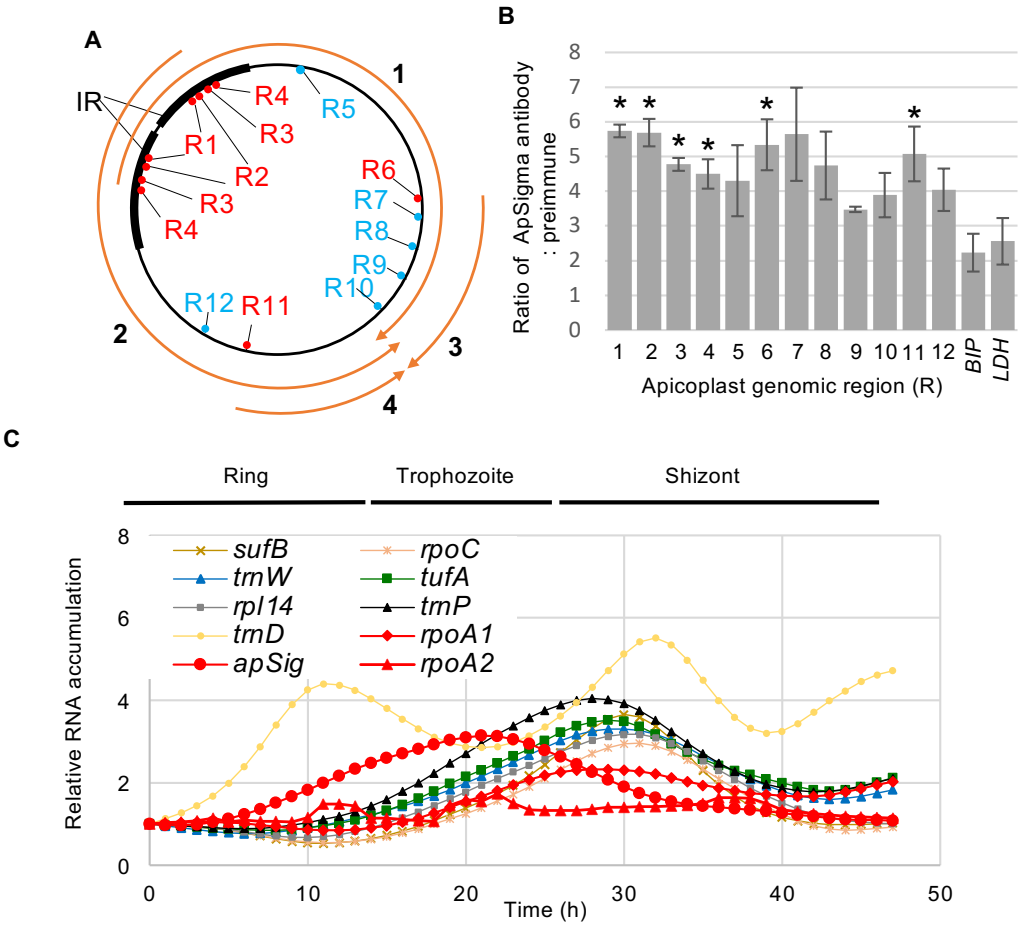
A
IR
R4
R5
R1
R3
R2
R6
R7
R3
R8
R4
R9
R10
R12
R11
1
2
3
4
B
Ratio of ApSigma antibody : preimmune
Apicoplast genomic region (R)
BIP
LDH
C
Ring
Trophozoite
Shizont
sufB
trnW
rpl14
trnD
apSig
rpoC
tufA
trnP
rpoA1
rpoA2
Relative RNA accumulation
Time (h)

Fig. 2

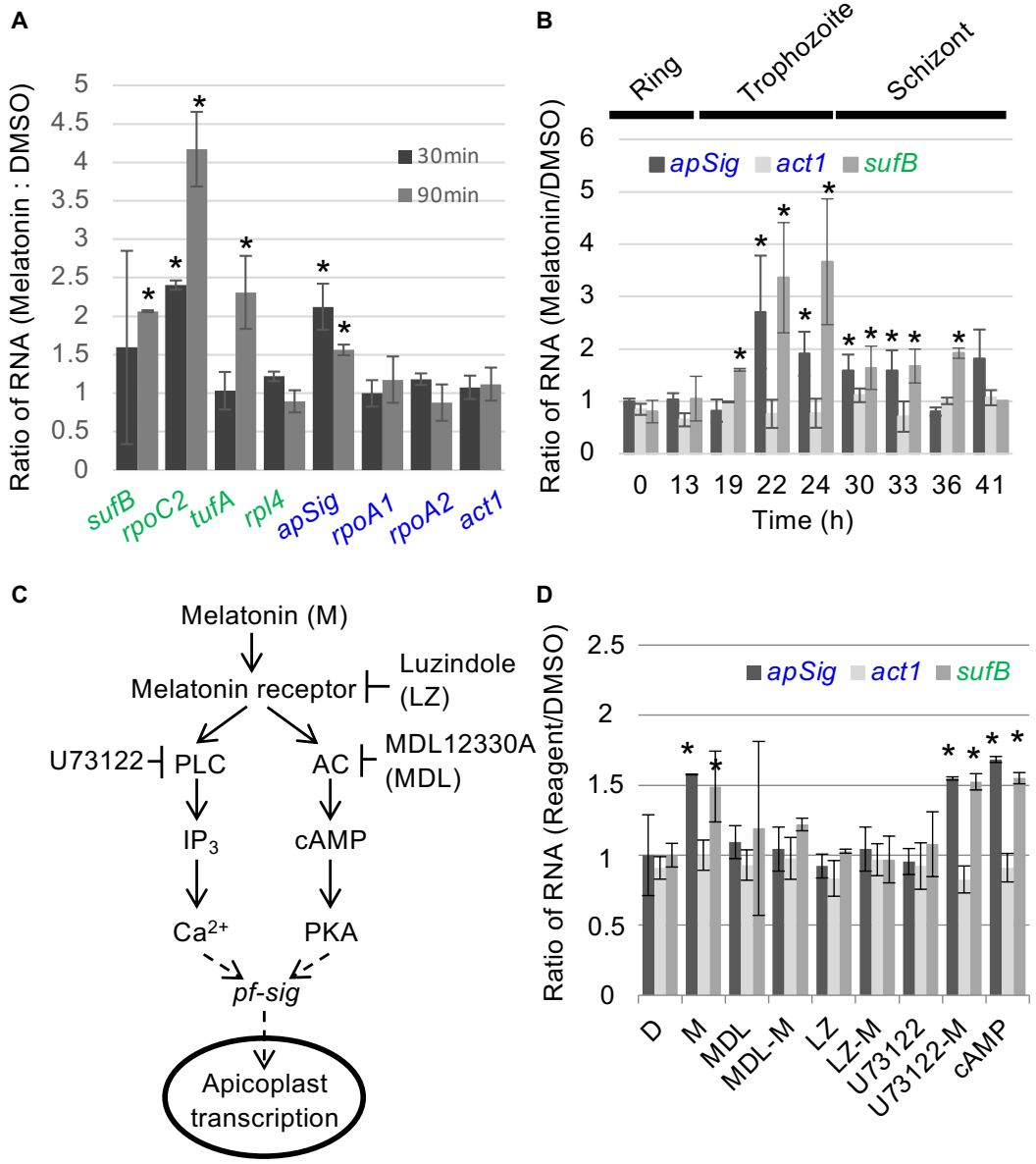
A
Ratio of RNA (Melatonin : DMSO)
30min
90min
sufB
rpoC2
tufA
rpl4
apSig
rpoA1
rpoA2
act1
B
Ring
Trophozoite
Schizont
Ratio of RNA (Melatonin/DMSO)
apSig
act1
sufB
Time (h)
C
Melatonin (M)
Melatonin receptor
Luzindole (LZ)
U73122
PLC
AC
MDL12330A (MDL)
IP3
cAMP
Ca2+
PKA
pf-sig
Apicoplast transcription
D
Ratio of RNA (Reagent/DMSO)
apSig
act1
sufB
D
M
MDL
MDL-M
LZ
LZ-M
U73122
U73122-M
cAMP

Fig. 3

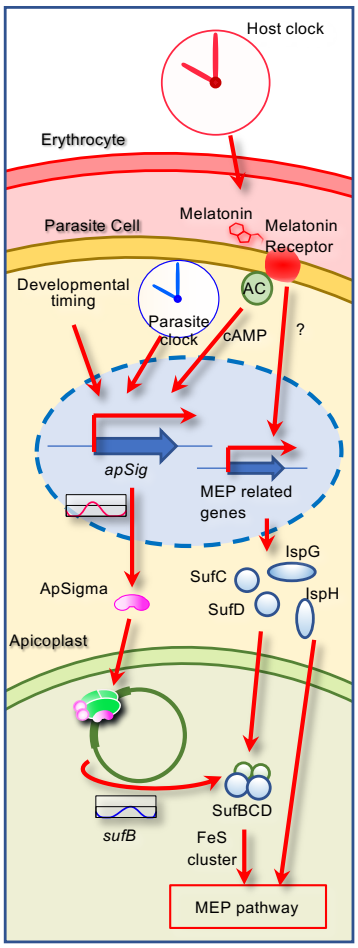
Host clock
Erythrocyte
Parasite Cell
Melatonin
Melatonin Receptor
Developmental timing
Parasite clock
AC
cAMP
?
apSig
MEP related genes
IspG
SufC
IspH
SufD
ApSigma
Apicoplast
SufBCD
sufB
FeS cluster
MEP pathway

Fig. 4